8th US National Combustion Meeting
Organized by the Western States Section of the Combustion Institute
and hosted by the University of Utah
May 19-22, 2013.

Methanol Droplet Combustion in Oxygen-Inert Environments in Microgravity

Vedha Nayagam[1], *Daniel L. Dietrich*[2], *Michael C. Hicks*[2]
Forman A. Williams[3]

[1]*National Center for Space Exploration Research, NASA Glenn Research Center, Cleveland, Ohio 44135*

[2]*NASA Glenn Research Center, Cleveland, Ohio 44135*

[3]*Department of Mechanical and Aerospace Engineering, University of California San Diego, La Jolla, CA 92093*

The Flame Extinguishment (FLEX) experiment that is currently underway in the Combustion Integrated Rack facility onboard the International Space Station is aimed at understanding the effects of inert diluents on the flammability of condensed phase fuels. To this end, droplets of various fuels, including alkanes and alcohols, are burned in a quiescent microgravity environment with varying amounts of oxygen and inert diluents to determine the limiting oxygen index (LOI) for these fuels. In this study we report experimental observations of methanol droplets burning in oxygen-nitrogen-carbon dioxide and oxygen-nitrogen-helium gas mixtures at 0.7 and 1 atmospheric pressures. The initial droplet size varied between approximately 1.5 mm and 4 mm to capture both diffusive extinction brought about by insufficient residence time at the flame and radiative extinction caused by excessive heat loss from the flame zone. The ambient oxygen concentration varied from a high value of 30% by volume to as low as 12%, approaching the limiting oxygen index for the fuel. The inert dilution by carbon dioxide and helium varied over a range of 0% to 70% by volume. In these experiments, both freely floated and tethered droplets were ignited using symmetrically opposed hot-wire igniters and the burning histories were recorded onboard using digital cameras, downlinked later to the ground for analysis. The digital images yielded droplet and flame diameters as functions of time and subsequently droplet burning rate, flame standoff ratio, and initial and extinction droplet diameters. Simplified theoretical models correlate the measured burning rate constant and the flame standoff ratio reasonably well. An activation energy asymptotic theory accounting for time-dependent water dissolution or evaporation from the droplet is shown to predict the measured diffusive extinction conditions well. The experiments also show that the limiting oxygen index for methanol in these diluent gases is around 12% to 13% oxygen by volume.

1 Introduction

Studies of droplet combustion are of interest from both fundamental and applied viewpoints, the latter in connection with both combustor performance and safety issues. Influences of carbon dioxide and helium, as well as increased nitrogen, in the atmosphere on the combustion characteristics and on extinction bear on questions of fire extinguishment. Liquid fuel droplets also are convenient vehicles for investigating relevant combustion processes from fundamental viewpoints, and

methanol, as a non-sooting fuel, offers an opportunity to examine an important simplified case. Although there have been a number of studies of methanol droplet combustion and extinction in the past, influences of different atmospheres are poorly understood. For these reasons, the present research is designed to advance our knowledge of methanol droplet combustion in such atmospheres. Extensive data of this kind on the combustion of methanol droplets have now been obtained in the FLEX program onboard the International Space Station (ISS). More than 100 droplets have been burned. Here we repost much of these new data and offer simplified analyses of the results.

Methanol droplet vaporization in a humid environment apparently was first studied by Law and co-workers in 1987 [1]. They showed that, when a methanol droplet vaporizes in a humid environment, water condenses on the cold droplet surface and is transported into the interior. The latent heat of water released during condensation was stated to increase the methanol vaporization rate. Subsequently, the combustion of methanol droplets in a quiescent microgravity environment [2, 3] and in free falling conditions [4] was investigated. Cho et al. [2] conducted methanol droplet-combustion experiments in helium-oxygen mixtures, chosen because extinction diameters could be accurately measured in a short-duration microgravity facility as a result of the increased burning rates produced by highly conductive helium mixtures. Yang et al. [3] also showed experimentally that pure methanol droplets burning in air exhibit extinction at a non-zero droplet diameter. Lee and Law [4] studied the combustion of freely-falling methanol and ethanol droplets and demonstrated that they absorb water produced during the combustion process. They also measured the water content of the droplet as a function of burning time and the extinction diameters for both methanol and ethanol droplets.

Droplets of initially pure methanol and methanol-water mixtures, diameters 2-5 mm, were burned in a space-shuttle experiment aboard Columbia during the USML-2 mission [5]. The results showed that for pure methanol, unlike the alkane droplets that were also studied on that mission, the extinction diameter varies linearly with the initial droplet diameter. Okai and co-workers [6], as a part of their methanol-dodecanol droplet-array experiments, measured the extinction diameter for a single methanol droplet at atmospheric pressure, and additional data from the USML-2 experiments has been reported and analyzed [7]. Marchese et al. [7] show that for small methanol droplet burning in air, radiation is unimportant, and the flames extinguish by diffusion-controlled mechanisms, similar to the diffusive-extinction results of the present study. They also show that when the initial droplet diameter is greater than roughly 4 mm, the droplet flame extinguishes through excessive radiative heat loss, as predicted in the analysis of Chao et al. [8]. More recently Hicks et al. [9] studied the influence of carbon dioxide dilution on methanol droplet extinction for a fixed oxygen concentration of 21% at one atmospheric pressure. They showed that the measured extinction diameter can be correlated well by a simplified theory that employs a critical Damköhler number.

Results of several theoretical and numerical studies of methanol droplet combustion which include water absorption, have been presented in the past [9–15]. One-dimensional numerical simulations [10] with detailed chemical kinetics for methanol showed that liquid-phase molecular diffusion of condensed water in the droplet interior is too slow to be consistent with the observed large amount of water present in the droplets during the experiments. It was concluded that convective transport within the liquid droplet must occur[10]. A reduced chemical-kinetic scheme for methanol gas-phase combustion chemistry was used to examine burning under two limiting conditions for

droplet internal mixing, namely a purely diffusive mode, and a fully mixed mode [11]. The results showed that the perfect liquid-phase mixing model predicts extinction diameters close to the experimentally observed values, and it was speculated that diffusocapillary (or solutal-Marangoni) instability, caused by the difference between the surface tension of water and that of methanol, could lead to strong internal circulation. Axisymmetric numerical simulations with surface-tension effects included have shown that this type of Marangoni effect in fact has a strong influence during methanol droplet evaporation and combustion [16–18]. Water absorption with a well-mixed liquid-phase thus is a reasonable approximation for describing methanol droplet combustion.

In a paper reporting somewhat more detailed theoretical model calculations [9], it was indicated in introductory considerations that simplified physical reasoning can be used to estimate the droplet diameter at extinction of combustion of an initially pure methanol droplet. During most of the combustion history, a fraction of the water produced in the flame diffuses back to the surface of the droplet, where it is readily absorbed, at an approximately constant rate controlled by gas-phase diffusion. This leads to a gradual increase of the water concentration in the liquid, and eventually that concentration becomes high enough that the equilibrium gas-phase water concentration at the droplet surface exceeds the water concentration at the flame, so that the direction of gas-phase water diffusion is reversed, and water begins to be transported out of the droplet rather than into it. This occurs when about 30% of the mass of the droplet is water, and the droplet then begins to burn as a binary mixture of methanol and water. The adiabatic flame temperature of this diluted mixture is, however, significantly less than that of pure methanol, actually below the temperature range, 1200 - 1700 K, that results in chemical-kinetic gas-phase flame extinguishment. Once outward water transport begins, therefore, the outward water flux rapidly increases and extinguishes the combustion, according to this simplified physical picture.

In this model, the extinction diameter then is approximately the droplet diameter at the end of the stage of water accumulation. This, however, is only a first approximation. Extinction conditions have been calculated more accurately by Rate-Ratio Asymptotic [11] and also numerically with detailed chemistry [14]. Recently, a simpler Activation-Energy Asymptotic (AEA) approach has been developed for the problem [15]. Here we exploit this simplified AEA approach further and apply it to the more extensive data that now exist. We also address droplet burning rates and flame standoff distances. The last two topics are addressed first, below, after the description of the experiment. Then the extinction conditions are considered in more detail. It will be seen that these simplified approaches can provide reasonable agreements with the experimental results, while improving understanding of the combustion processes. The success of the AEA approach, in this context, indicates that early [19] one-step empirical overall reaction-rate parameters, developed from counterflow combustion experiments, can been applied remarkably well in droplet combustion.

2 Experiments

The experiments were conducted using the Multi-User Droplet Combustion Apparatus (MDCA) installed in the Combustion Integrated Rack (CIR) facility in the US Module of the ISS. The cylindrical combustion chamber in the CIR has a free-volume of approximately 95 liters with the MDCA insert installed. The MDCA used an opposed-needle deployment technique to freely

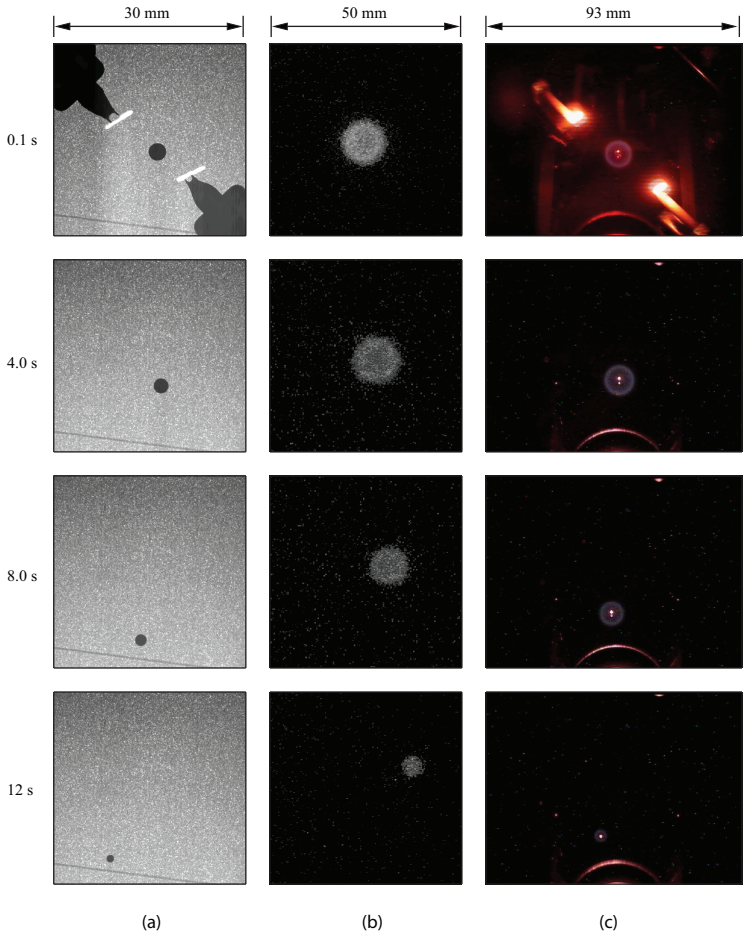

Figure 1: Typical images from FLEX experiments for methanol burning in air at 1 atm pressure: (a) back-lit droplet image, (b) UV-image of the flame, and (c) Color camera image of the flame. Image scale and time after ignition are also shown. Droplet initial diameter was 2.75 mm.

deploy droplets of chosen size in microgravity. Sometimes the droplet was tethered using a small silicon carbide (SiC) fiber to keep it in the field of view of the cameras. Ignition of the deployed droplet was accomplished using two symmetrically positioned hot-wire igniters. The experimental diagnostic system consisted of a black-and-white, back-lit droplet image capture camera, a UV-sensitive flame imaging camera filtered to observe OH*-chemiluminescence at 310 nanometer wave length, and a CCD color camera with a wider view angle. All the camera images were obtained at 30 frames per second and digitally stored on-board the CIR and down-linked at a later time for analysis. The color camera with its real-time down-link capability is also used to conduct experiment operations from the ground at the Telescience Support Center located in NASA Glenn Research Center. Prior to an experimental run, the Fuel and Oxidizer Management Assembly (FOMA) system of the CIR is used to fill the combustion chamber with the desired ambient gas mixture consisting of oxygen, nitrogen, and carbon dioxide at a selected pressure. Typically several droplet burns were performed in each environment before venting the combustion chamber to space vacuum and refilling. Further details of experiments and operational procedures can be found in Dietrich et al [20].

3 Results

Over one hundred methanol droplet tests in varying diluent concentrations and at primarily two different ambient pressures (0.7 and 1 atm) have been performed to date. In these tests the oxygen concentration varied from 30% to 12% by volume while the carbon dioxide and helium diluent concentrations varied in the range of 0% to 70% by volume and the rest of the inert was nitrogen. The initial droplet diameter varied between 1.5 mm and 4.5 mm. A representative set of observations from the three different cameras are shown in Fig. 1. From the digital images the droplet diameter D and the flame diameter D_f were measured as a function of time using a commercially available image analysis software package. The flame diameters obtained from the color camera typically fell slightly below the UV-camera measurements. Since the resolution of the UV-camera was better than the color camera we report here only the UV-camera measurements for flame size.

3.1 Burning Rates

Figure 2 shows droplet diameter-squared and the flame diameter plotted as functions of time for three different cases. Run #204 corresponds to a methanol droplet of initial diameter 2.75 mm burning in air (20% O_2 and 79% N_2) at one atmospheric pressure. The slope of the D^2 versus time curve is fairly linear through most of the burning period except toward the end where the slope decreases slightly prior to flame extinction, which occurs at a droplet diameter of 1.10 mm, called the extinction diameter D_e. Run #110 corresponds to a droplet with an initial diameter of 2.83 mm burning in 21%O_2 and 30% CO_2 environment whereas run #263 had an initial diameter of 2.67 mm and an atmosphere consisting of 21% O_2 and 30% He with the remaining diluent being nitrogen in both cases. The ambient pressure for both of these cases was 0.7 atm. It can be seen from the slopes of the D^2 versus time curves in figure 2 that substituting carbon dioxide with helium leads to a higher burning rate due to the increased thermal conductivity of He compared to CO_2 and consequently a smaller burning time for droplets of similar size. The extinction diameters D_e for run #110 and #263 were 1.57 mm and 1.42 mm, respectively. For these two cases the droplet remains in the field of view after flame extinction and the continued evaporation at a much slower rate in the hot atmosphere can be seen in the D^2-versus-time curves. It is also interesting to note that for all three cases the flame diameter initially increases and then decreases to a smaller value at extinction, showing that the extinction is caused by insufficient residence time rather than radiative heat loss from the flame.

Figure 3 shows a compilation of all measured burning-rate constants $K_{ex} = -d(D^2)/dt$, plotted against corresponding calculated burning-rate constant K_{cal} based on classical quasi-steady theory, namely

$$K_{cal} = 8\frac{\lambda_g}{\rho_l c_{Pg}} \ln(1+B), \tag{1}$$

where λ_g and c_{Pg} are the thermal conductivity and specific heat of the gas mixture, respectively, ρ_l is the density of the liquid, and B is the transfer number. The transfer number B is expressed as

$$B = \frac{q_f Y_{O,\infty} f + c_{Pg}(T_\infty - T_b)}{L}. \tag{2}$$

In the above equation $Y_{O,\infty}$ is the ambient oxygen mass fraction, q_f is the heat of combustion per unit mass of the fuel, L is the heat of vaporization of the liquid fuel, and f is the stoichiometric

fuel-to-oxygen mass ratio. The fuel boiling point is T_b, and the ambient temperature is T_∞. The property values needed in equation (1) and (2) are evaluated according to the semi-empirical recipe proposed by Law and Williams [21].

The experimental K_{ex} values were obtained by linear least-square fitting of the D^2-versus-time curves. Only the middle 80% of the droplet lifetime was used in these curve-fits, to avoid the initial heat-up period and the later non-linear behavior close to extinction. The size of each data point in Fig.3 is proportional to the initial droplet size D_0. It is interesting to note that the smaller droplets have a higher burning-rate constant than the classical quasi-steady prediction. This is understandable because extinction occurs early for smaller droplets when water condensation is predominant, and the resulting condensation heat release enhances the burning rate. For larger droplets, extinction takes place at a later stage when water evaporation becomes influential and negates any gains in burning rate experienced during the earlier condensation period. Clearly, the quasi-steady theory used to calculate K_{cal} does not include these unsteady water-absorption effects. Although it is possible to improve the correlation shown in Fig. 3 by including such effects in estimating K_{cal}, for example using the unsteady AEA model discussed later, this is not attempted here because of the fairly substantial scatter in the experimental data from run to run.

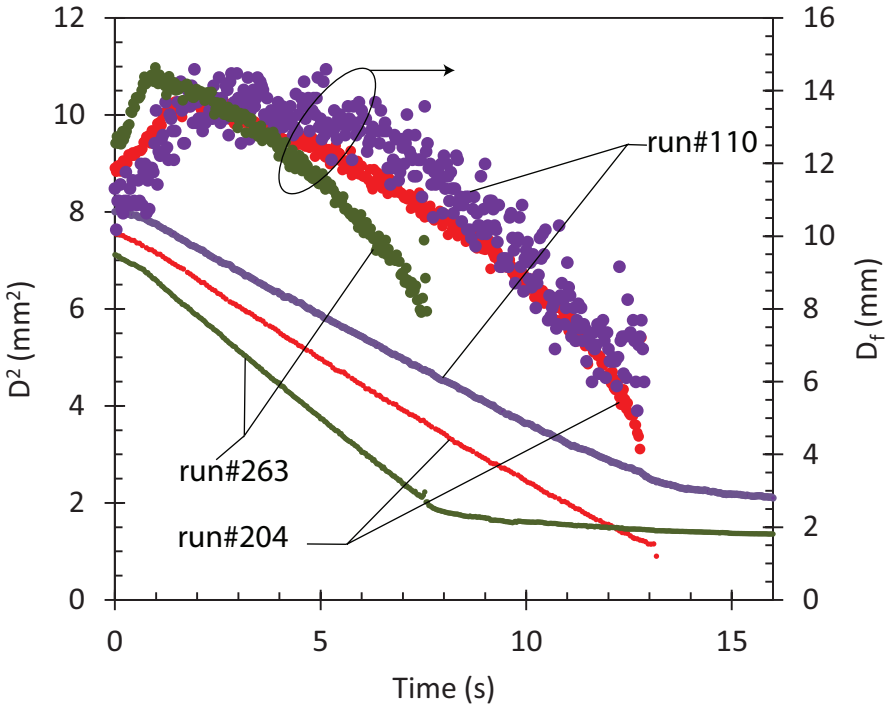

Figure 2: Droplet diameter square D^2 and flame diameter D_f as a function of time for three free-floated droplet tests: Run#110 21% O_2 and 30% CO_2 at 0.7 atm; Run# 204 21% O_2 and 79% N_2 at 1 atm; Run# 263 21% O_2 30% He and 49% N_2 at 0.7 atm.

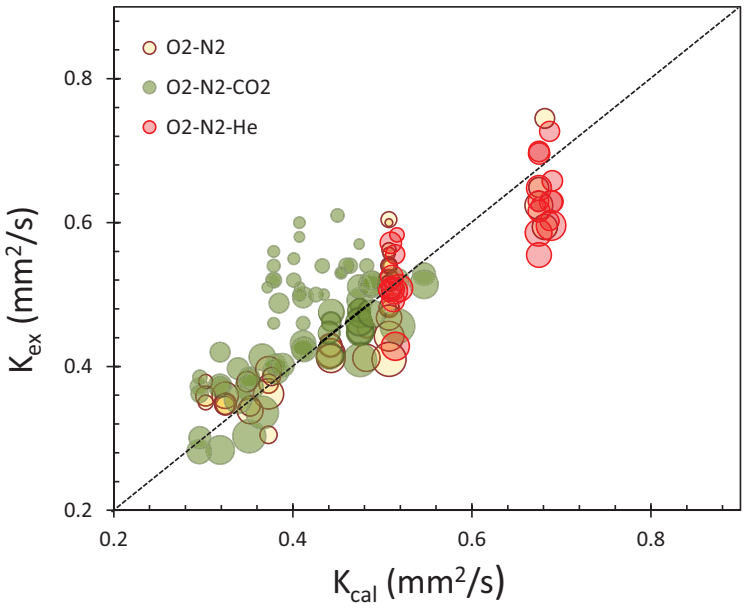

Figure 3: Measured burning-rate constant K_{ex} versus calculated burning-rate constant K_{cal} in different diluent-substituted environments: the size of the bubble is proportional to the droplet initial diameter.

3.2 Flame-Standoff Ratios

The classical quasi-steady theory of droplet combustion predicts that the ratio of the flame diameter to the droplet diameter, D_f/D, is a constant, independent of the droplet initial size, for a given environmental condition, and it typically yields a value several times that of experimental measurements. Here we compare the measured flame-standoff ratios against the predictions of a recently developed simplified theory [22] that takes into account the effects of water absorption and employs an effective diffusion coefficient for oxygen. According to [22] the flame-standoff ratio is given by the expression

$$\frac{D_f}{D} \approx \frac{1}{2}\left[a + \sqrt{a^2 - 2a + 4b + 1} + 1\right], \tag{3}$$

where,

$$a = \left(\frac{W_{av}\nu_o\rho_f K}{8W_f\nu_f\rho_g\alpha_o}\right)\frac{1}{x_{o,\infty}}, \text{ and } b = \frac{W_w\rho_f}{W_f\rho_w}\frac{\nu_o\alpha_w x_{w,f}}{\nu_f\alpha_o x_{o,\infty}}. \tag{4}$$

Here ρ_g is the gas density, $\rho_f$is the liquid fuel density, ρ_w is the water density and W_{av} is the average molecular weight of the gas-phase species, W_f and W_w are the molecular weights of fuel and water, respectively, $x_{o,\infty}$ is the ambient oxygen mole fraction and $x_{w,f}$ is the water mole fraction at the flame, ν_f and ν_o are the molar stoichiometric coefficients for fuel and oxygen for a one-step reaction. The effective diffusion coefficients of water vapor and oxygen are denoted by α_w and α_o, respectively, and K is the burning-rate constant obtained from experiments.

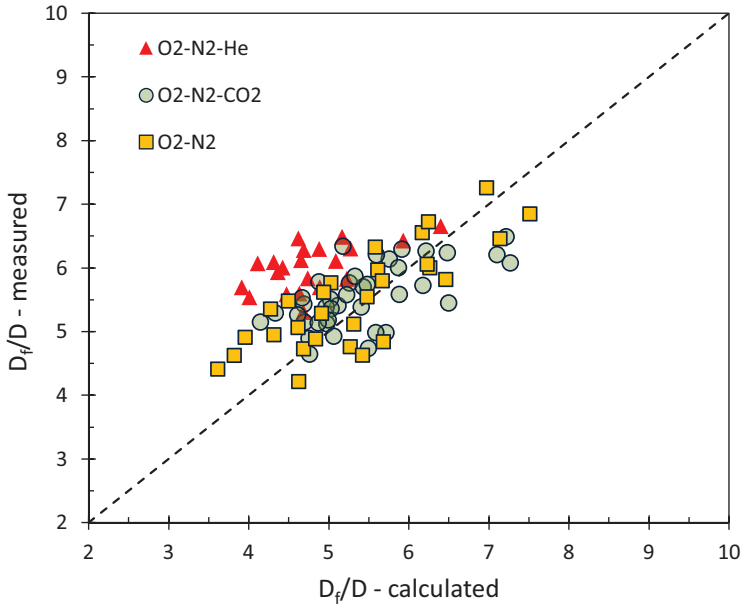

Figure 4: Calculated and measured flame-standoff ratios in different diluent-substituted environments.

Figure 4 shows measured flame-standoff ratios (FSR) plotted against the calculated values obtained from Eqn. (3). The measured FSRs are obtained by plotting instantaneous flame standoff ratios as a function of time and identifying an average value during the quasi-steady burning period where it remains relatively constant. Environments under which the flame does not reach a quasi-steady condition, such as those at low ambient oxygen concentrations, are excluded from Fig. 4. Considering the number of independent parameters involved, namely different initial droplet diameters, various oxygen and diluent concentrations, the simplified theoretical model predicts the flame-standoff ratio reasonably well. However, Fig. 4 suggests a systematic disagreement for different diluent mixtures. The measured FSRs for $O_2 - N_2 - He$ mixtures are consistently higher than the predicted values compared to the $O_2 - N_2 - CO_2$ mixture data points. While the exact reason for this discrepancy is not clear at this point, and further work is needed to understand this behavior, it is worthwhile to point out here that the simplified model described in [22] is a quasi-steady model with water mass flux estimated employing a fixed value of the water mole fraction at the flame $x_{w,f}$ and zero at the droplet surface, which may not be an accurate assumption under varying oxygen and diluent concentrations.

3.3 Flame Extinction

As described earlier, during methanol droplet combustion the flame can extinguish itself by two different mechanisms. First, the flame can extinguish as it moves closer to the droplet surface due to insufficient residence time ("diffusive extinction"); this generally occurs toward the end of the combustion period as the flame shrinks in size. The second mechanism is the excessive radiative heat loss from the flame as it grows in size, and this mechanism reduces the flame temperature

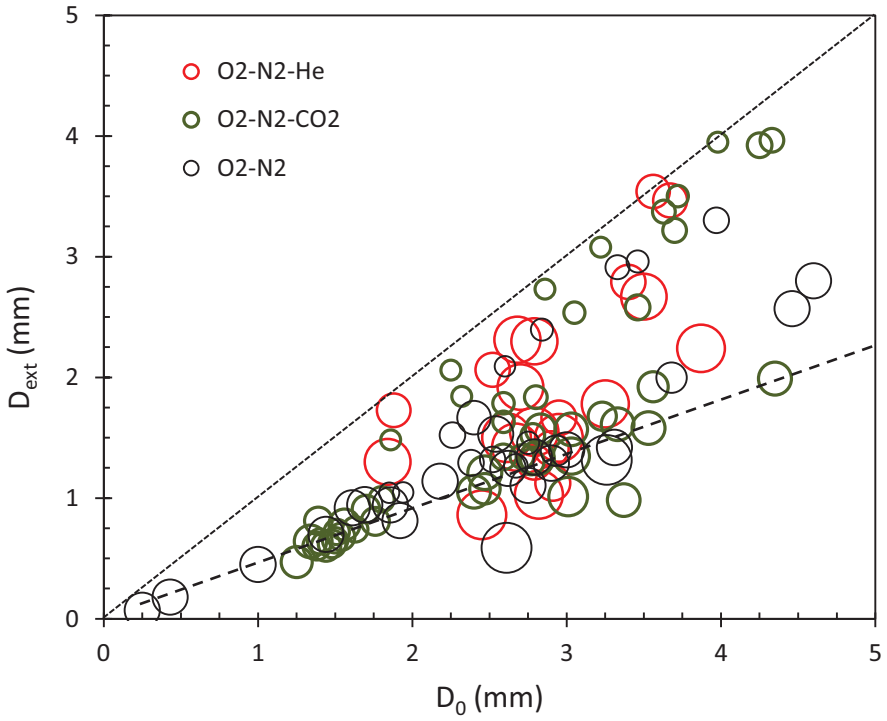

Figure 5: Methanol droplet extinction diameter versus initial droplet diameter in diluent-substituted environments: the size of the bubble is proportional to ambient oxygen mole fraction.

to sufficiently low values for the flame to go out ("radiative extinction"); this process is generally observed for larger droplets at lower oxygen concentrations when the flame is large in size and lies farther away from the droplet surface. Flame extinctions in both modes were observed during the FLEX tests, and the results are summarized in Fig. 5, where the extinction diameter D_e is plotted against the initial diameter D_0. This figure contains over 100 data points, covering a range of oxygen concentration, CO_2 and He diluent concentrations, and initial droplet sizes, at two different pressure. In the legend the points are grouped into only three different categories, according to the diluent present, for simplicity. The size of the data point is proportional to the oxygen mole fraction of the test in this figure. Despite the lumping together of some of the independent variables, the figure clearly shows two different trends. As expected, the larger droplets at lower oxygen concentrations (smaller circles in figure) fall closer to the 45° line, showing that the droplet extinguishes rather quickly after ignition through radiative heat loss. At smaller droplet sizes, the data fall approximately along a straight line, irrespective of the diluent concentrations. The dashed line provides an approximate correlation of these diffusive-extinction results in Fig. 5.

It is worthwhile to compare the experimentally determined extinction diameters with simplified theoretical predictions. Figure 6 shows such a comparison for air at one atmosphere. The predictions of rate-ratio asymptotics (RRA) [11], of the recently developed activation-energy asymptotics (AEA) [15], and of numerical simulation using detailed chemical kinetics [14] are also shown in the figure (see the lower curves). In contrast to selecting the product of density and diffusion coefficient, ρD, to match the experimental burning rate and fitting one particular experimental extinction

point to determine an appropriate heat capacity [15] for the AEA computation, here an entirely *a priori* approach is adopted instead. The prescription of Law and Williams is used to determine ρD, as was done in the earlier burning-rate calculations, and the value of a c_P was selected such that the quasi-steady flame temperature matches the adiabatic flame temperature for the pure fuel in the air environment. This procedure renders the AEA model fully closed and consistent in the sense that there is no calibration involved. The resulting line, marked AEA in Fig. 6, is seen to be close to the RRA and numerical predictions, all of which lie below the data. Since the extinction, however, occurs after absorbed water begins to evaporate from the droplet, the appropriate adiabatic flame temperature is below that for pure fuel. To obtain an idea of the magnitude of this effect, the C_P values were increased by 60% so that the adiabatic flame temperature was around 1700 K, and the resulting prediction of the AEA theory then lies much closer to the experimental data as shown by the line marked AEA-2. Because of the expected increase in droplet water content at extinction with increasing initial droplet diameter the relevant adiabatic flame temperature likely decreases with increasing D_0 thereby causing the slope of the experimental points in Fig. 6 to exceed that of AEA-2 line. These observations suggest general approximate agreement between experiment and computation for extinction diameters.

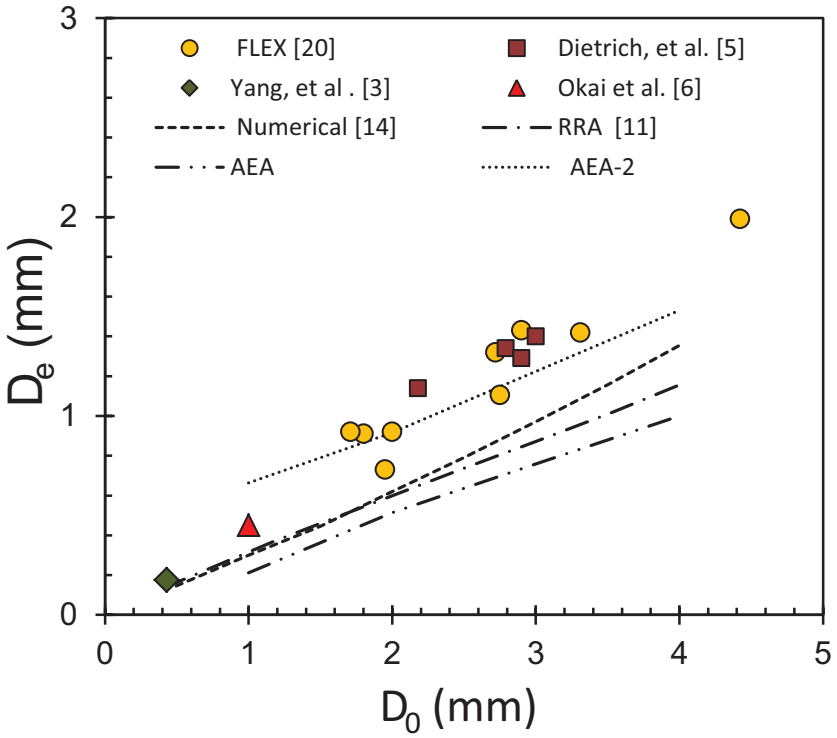

Figure 6: Methanol droplet extinction diameter versus initial diameter for air: Comparison between experiments and different theories.

4 Conclusion

Extensive experimental results for burning-rate constants, flame-standoff ratios, and extinction diameters during methanol droplet combustion in oxygen-nitrogen, oxygen-nitrogen-carbon dioxide,

and oxygen-nitrogen-helium mixtures in microgravity have been obtained. It was shown that simplified theoretical models can correlate the burning rate and the flame-standoff ratios reasonably well, although further investigations notably concerning the latter, seem warranted. The extinction-diameter prediction by activation-energy asymptotics, while showing correct trends, need more considerable further improvement. The results reported here can provide a basis for future improvements in descriptions of methanol droplet combustion.

Acknowledgments

This work was supported by the NASA Space Life and Physical Sciences Research and Applications Program and the International Space Station Program. We would like to thank our other FLEX team members, C.T. Avedisian, M.Y. Choi, F.L. Dryer, and B.D. Shaw for their support.

References

[1] C.K. Law, T.Y. Xiong, and C.H. Wang. *Int. J. Heat Mass Transfer*, 30 (1987) 1435–1443.

[2] S.Y. Cho, M.Y. Choi, and F.L. Dryer. *Proceedings of the Combustion Institute*, 23 (1990) 1611–1617.

[3] J.C. Yang, G.S. Jackson, and C.T. Avedisian. *Proceedings of the Combustion Institute*, 23 (1990) 1619–1625.

[4] A. Lee and C.K. Law. *Combustion Science and Technology*, 86 (1992) 253–265.

[5] D.L. Dietrich, J.B. Haggard Jr., F.L. Dryer, V. Nayagam, B.D. Shaw, and F.A. Williams. *Proceedings of the Combustion Institute*, 23 (1996) 1201–1207.

[6] K. Okai, O. Moriue, M. Araki, M. Tsue, M. Kono, J. Sato, D.L. Dietrich, and F.A. Williams. *Combustion and Flame*, 121 (2000) 501–512.

[7] A.J. Marchese, F.L. Dryer, and R.O. Colantonio. *Proceedings of the Combustion Institute*, 27 (1998) 2627–2634.

[8] B.H. Chao, C.K. Law, and J.S. T'ien. *Proceedings of the Combustion Institute*, 23 (1990) 523–531.

[9] M. C. Hicks, V. Nayagam, and F. A. Williams. *Combustion and Flame*, 157 (2010) 1439–1445.

[10] A.J. Marchese and F.L. Dryer. *Combustion and Flame*, 105 (1996) 104–122.

[11] B.L. Zhang, J.M. Card, and F.A. Williams. *Combustion and Flame*, 105 (1996) 267–290.

[12] B.L. Zhang and F.A. Williams. *Combustion and Flame*, 112 (1998) 113–120.

[13] T. Farouk and F.L. Dryer. *Combustion and Flame*, 159 (2012) 200–209.

[14] T.I. Farouk and F.L. Dryer. *Combustion and Flame*, 159 (2012) 3208–3223.

[15] V. Nayagam. *Combustion and Flame*, (submitted, 2013) .

[16] H.A. Dwyer, A. Aharon, B.D. Shaw, and H. Naizmand. *Proceedings of the Combustion Institute*, 26 (1996) 1613–1619.

[17] H.A. Dwyer, B.D. Shaw, and H. Naizmand. *Proceedings of the Combustion Institute*, 27 (1998) 1951–1957.

[18] V. Raghavan, D.N. Pope, and G. Gogos. *Combustion and Flame*, 145 (2006) 791–807.

[19] K. Seshadri and F.A. Williams. Effect of CF_3Br on counterflow combustion of liquid fuel with diluted oxygen. In Gann R. G., editor, *Halogenated Fire Suppressants*. American Chemical Society, Washington, D. C., 1975.

[20] D. L. Dietrich, P.V. Ferkul, V.M. Bryg, V. Nayagam, M.C. Hicks, F.A. Williams, F.L. Dryer, B.D. Shaw, M.Y. Choi, and C.T. Avedisian. Detailed results from the flame extinguishment experiment (FLEX). Technical Publication NASA/TP-2013-216046, NASA, Glenn Research Center, Cleveland OH 44135, USA, 2013.

[21] C.K. Law and F.A. Williams. *Combustion and Flame*, 19 (1972) 393–405.

[22] V. Nayagam. *Combustion and Flame*, 157 (2010) 204–205.